LUPINE PUBLISHERS

Current Trends in Computer Sciences & Applications

DOI: 10.32474/CTCSA.2023.03.000151

ISSN: 2643-6744

Research Article

Design And Implementation of Train Independent Electromagnetic Self-Driving-Fed Energy Storage Wheel Based on FPGA

Yubo Wang*

Department of Electrical and Mechanical Engineering, Innovation Research Institute of CETC Taiji Computer Corp, China

***Corresponding author:** Yubo Wang, Department of Electrical and Mechanical Engineering, Innovation Research Institute of CETC Taiji Computer Corp, China

Received: July 19, 2023 **Published:** July 28, 2023

Abstract

This paper studies the integration of railway transportation system monitoring equipment and the operation of each component, and usually completes the equipment design and software development for the production and operation of the main components by combining DSP and FPGA and understands the application of troubleshooting. With reference to the automatic electromagnetic two-wheeled vehicle, this article analyzes the vehicle based on the structure of 7 degrees of freedom and the physical calculation of the DC vehicle, including weight distribution control and weight production control. Independent electromagnetic self-driving system. The driving control distribution system takes the power of the vehicle as the target range, obtains the speed and the center of rotation in the digital range as the target control limit, and uses the error between the actual value and the expected value as the target value. Changing the control and releasing the required vehicles is the direction in terms of transparency control. According to the expected value of the travel speed, the performance of the car is allocated. The energy filter of the fed-type energy storage device has low power consumption, simple structure and fast realization speed. It can not only improve the driving performance of the car, but also convert part of the mechanical energy of the car into electric energy, which is one of the research fields. In view of this, this article studies the structure of the equipment circuit, and briefly introduces the configuration of the equipment and the DSPACE software control system. Complete automobile wheel design and energy storage system, mainly including production and design of semi-active control circuit, chip selection and design of expansion circuit; fuel storage design, energy storage design, selection management analysis, electrical principle design and analysis of stable command circuit.

Keywords: FPGA; Independent Electromagnetic Self-Drive; Fed Energy Storage; Wheel Design

Introduction

Automated electromagnetic autonomous electric vehicles have many benefits in reducing environmental and energy problems and improving vehicle performance. The center of the wheel ensures the stability of the car's operation. In view of this, this paper studies and studies the electromagnetic two-wheel drive control system for self-driving electric vehicles. Therefore, this article first defines the basic design of the DSP for linear data processing and the basic design of the FPGA for remote control and selects the floating DSP TMS320C6713 and Cyclone III series FPGAEP3C16 according to the requirements of discovery and processing. At the same time, F256 pointed out that the link between DSP and FPGA realized the EMIF bus to transmit data, and the UART bus to transmit data. Secondly, the configuration of the digital and analog circuits of the circuit board has been completed, including equipment repair circuits, minimum system circuits, storage circuits, communication circuits, etc., as well as PCB and wiring models. Finally, FPGA software components are developed from IP-based adapters and SOPC systems based on Nios II soft processors. The development of the remote driver is done

in language C and implemented in the basic operating system lxC/OS-II. Usage: For DSP software, it is recommended to use the second startup program and fast Flash format and introduce known FPGA communication and error diagnosis algorithms. Today, the concept of energy storage technology is mainly aimed at suspension, but due to its low cost, low energy consumption, easy control, and long service life, the suspension of energy-saving products has attracted attention from the automotive engineering community at home and abroad. As the most important part of the whole system, the semi-active suspension control system of fed-type power storage controls the generation of electromagnetic energy in the direct machine. The imposed characteristics directly affect the active production and suspension of semi-active products. Therefore, the design of semi-active control system is more important. This paper analyzes and designs a two-wheeled electromagnetic self-driving car based on the type of stored energy and incorporates the design work into an energy-saving car. Nowadays, research on the energy response path of energy storage suspension systems is limited to super capacitors, and obviously there are no other applications or recovery energy storage plans for super capacitors. Based on the influence of the operating characteristics of the semi-active system on the energy efficiency of the entire energy feed system, this topic proposes an energy storage system, which has important significance for the use and energy storage of electric vehicles in the future (including super Capacitor circuit loop and battery charging system).

Related work

Literature studied the linear transmission system of linear tracking equipment and the function of each component [1]. First, complete the design of the equipment, and then develop software to produce and run large-scale integrated trunk lines. The equipment failure detection system is used in rail transit [2]. Literature deeply analyzes the driving force as the control object, uses motion control strategy, based on the short-term control of the vehicle control system; the brushless DC loop motor control output unit is the most important unit [3]. Literature established a comparative circuit including DC power system, power storage system, ground power system and multi-track operating system with metal resistance and can clearly identify the relationship between energy flow and train operating conditions. The test results of Metro City Stone Lines verified the accuracy of the samples [4]. It is based on this research that affects the factors that modify the braking force distribution. Literature designed the whole system and built a single-leg suspension based on semi-functional control measures and landfill control strategy [5]. The energy response characteristics of the system were simulated and analyzed by MATLAB, and the preliminary selection of energy storage devices was completed [6]. The characteristics of the smoke system and the working characteristics of the semi-active control circuit are analyzed, and the change of the energy feed penalty for the working mode of the semi-active control circuit is obtained [7]. Literature is an alternative to multi-port Ethernet for subways [8]. It not only supports 100M transmission speed and dry Ethernet ports, but also provides four different types of Ethernets to carry VoIP voice services, demanding video streams and other requirements [9].

The Design and Implementation of an Independent Electromagnetic Self-Driving System for Trains Based on FPGA.

The Overall Design of the Electromagnetic Self-Driving Subsystem

The vehicle torque control system (shown in Figure 1) is based on controlling the target force of the vehicle. Take the yaw value and the sliding side of the center density as the target and use the two-degree-of-freedom type vehicle to calculate the expected value of the target boundary. The true value of the numerical yaw can be obtained by answering the car model [10]. Built-in central sliding angle monitor, the exact value of Get is the center of the rotation angle; enter the amount of error between the actual value and the “best two” limit motion value to establish the time required for the car, as well as the estimated total power consumption, and distribution the number of trams and cars [11-12]. The whole control system consists of three parts: the target control limit of the system is created, the yaw minute control based on the clutch control and the driving force distribution module [13]. The main function of torque control based on emotion control is to generate the time required for the error e(B) on the slip side of the center density and the error e(y) of the digital scale. The e(B) and e(y) of the target layer control system are used as control output, and a small Mz1 torque is obtained under the condition of crazy car operation. After preventing ground collision, the output can ensure the stability of the vehicle. Mz is the required roll time [14]. Fuzzy control is a dual-production product structure, which directly uses the Mamdani algorithm for negative analysis. Through the medium torque method, the speed of the vehicle can be ascertained, and the Mz time of the vehicle that maintains a strong driving can be obtained [15].

Design of Electromagnetic Torque and Motor Equation of Motion

According to the analysis of the motor energy transmission method, a small part of the motor energy is produced by the loss of copper and iron, and most of the electrical energy is converted into constant magnetic energy. The torque function of the permanent magnet, namely electromagnetic power, electromagnetic energy can convert power and phase into electrical energy. It can currently be expressed as:

Regardless of various losses, consider completely converting electromagnetic power into energy to drive the rotor, namely:

Then:

Where: Q is the mechanical angular velocity of the motor.

The motion equation of the motor:

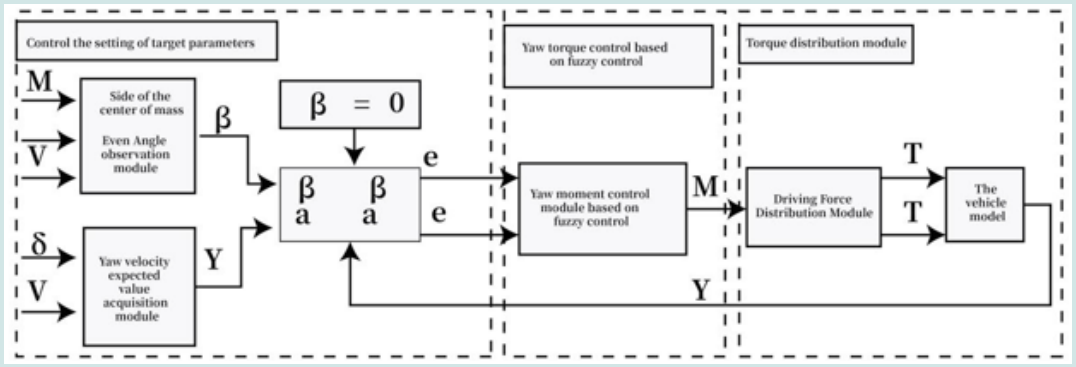

Figure 1: Schematic diagram of the structure of the train driving force distribution module.

Where;

TL-load torque;

J is the moment of inertia of the rotor;

BV is the coefficient of viscous friction.

The modification of Laplace's formula adopts:

FPGA Selection

FPGA Preliminary Selection

Although CPLD has many advantages, for example, no power supply will not lose data, no configuration tools, good confidentiality, shorter plans and production plans, and the ability to use fast power supplies, FPGAs are slower. Poor resource flexibility and low integration [16]. The main manufacturers of FPGAs are Altera, Xilinx, Lattice, Actel and Atmel. Among them, Xilinx is an innovative FPGA that provides more than half of the global market share. Altera is the ancestor of smart devices that can be used for programming, as well as an advocate and leader of global SOPC solutions. Altera combines real-time technology that can be applied to software tools with nuclear technology with intellectual property rights, making it easier for developers and designers [17]. The performance of FPGAs from major manufacturers is also different. For example, FPGAs from manufacturers such as Altera and Xilinx are based on Sram and have functions that limit programming time and compatibility [18]. It is suitable for public use and has many uses. Actel's FPGA uses a Flash or anti-fuse-based system, so it is very sensitive and is particularly suitable for military products with fewer users [19].

Logic Unit Estimation

Logic unit estimation is an important part of selecting FPGAs, and the methods for evaluating FPGAs from different vendors are also different [20]. The logic element Altera FPGA contains four search tables and D flip-flops. If users choose to use FPGAs by estimating the number of gates in smart components, they must match their design with digital circuits. Obviously, this method has a certain degree of difficulty [21].

FPGA Circuit Design

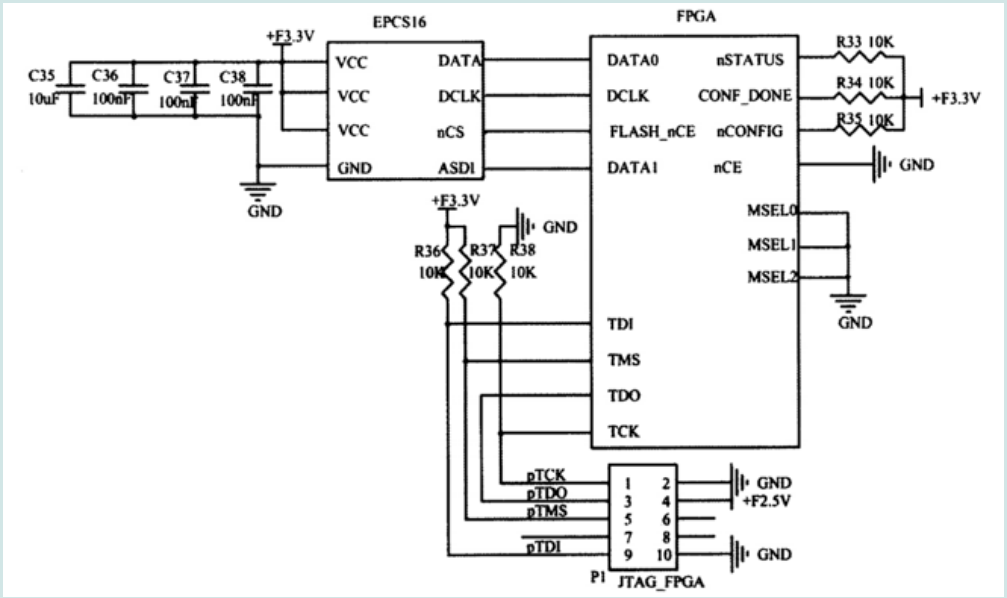

Figure 2: FPGA configuration circuit.

FPGA Minimum System

a) Download circuit.

The most commonly used import methods in the Cyclone III series include a series of active preventive measures, active parallelism, indirect chaining, active parallelism, and JTAG. Generally speaking, FPGA development board has two download files AS and JTAG. The design uses only JTAG to minimize the PCB area where interactions are most common. The JTAG format does not require the program to enter the configuration package but is a linear error of the operating program. At the same time, the program can be written into the configuration part 3 and 4 through the Flash download tool, which can meet the need for program deletion. FPGAs based on Sram technology also need external configuration tools. Altera provides a series of Flash programs for its FPGA software. See Figure 2

b) Clock circuit

An active oscillator called a crystal oscillator is used as a clock to charge the FPGA and is connected to the receiving pin of the FPGA.

FPGA Memory Circuit

The FPGA component uses an SD card to store the calculation results. SD cards have two modes: SDIO and SPI. However, when choosing SDIO mode, always need to select a controller with SDIO function mode. Considering that the Nios soft core is easy to read and write SPI format in this format, this design uses the SPI format of the SD card. Table 1 shows the SD card definition in SPI format. At the same time, both the SD card and FPGA IO port are compatible with 3.3V, and the following SDIO function verification is considered. Among them, pSD_CD is used to determine whether the SD card is inserted into the card slot.

Table 1: SD card SPI mode pin definition.

Pin number	Pin name	Pin function
1	#CS	Chip Select
2	DI	data input
3	Vss	Power ground
4	VDD	power supply
5	SCLK	clock
6	VSS2	Power ground
7	DO	Data output
8	RSV	Keep
9	RSV	Keep

Design and Implementation of Train-Fed Energy Storage Wheels

Control Strategy of Supercapacitor-Fed Energy Storage Wheel System

This article proposes to bring it into the grid as a control product to determine the grid lines and the information to be input and output. After the train enters the station, when the train is in braking mode, it is in the engine state and released to the network. The Udc power supply increases to reach the set Uup amount. After the power storage device is activated, the energy storage device is in the charging state BUCK, and energy from the grid of the super capacitor device is saved. The energy storage device draws energy from the grid and charges the current converter. The USC-Max of IL and return voltage is xakameynayaa looga, which can prevent excessive electric energy transmission and electric energy storage equipment damage; after the train leaves the station, the energy is removed from the network, resulting in the reduction of Udc power supply and Udc power network. After setting the Udown value, the electrical storage device will be turned on, and the energy storage device will be in production mode. At the same time, I still replace looga with fluid from USC voltage from the equipment to prevent excessive fluidity and excessive release rate from damaging the energy storage device. Train departure information and power generators have been adopted to avoid lowering the voltage network due to defects or other reasons, resulting in incorrect control. The concrete system is shown as in Figure 3.

Determination of the Main Parameters of the Energy Storage Feedback Converter Circuit

According to the analysis of energy storage energy conversion, the operating status of municipal trains can be divided into three categories: the operating status of energy storage response, the operating status of energy storage release, and the normal operating conditions of resistance control. When designing energy storage equipment, the energy storage equipment should have three different working areas to ensure that the energy storage equipment can work normally under three different working conditions. When analyzing the topology of the energy storage device in 3.2, the reverse converter DC/DC converter was finally selected as the bidirectional DC/DC circuit breaker. According to the operation requirements of urban railways, the DC/DC dual

transformers are reasonably designed to perform a complete energy-saving response. The entire circuit is shown in Figure 4, usually composed of four components: C capacitor filter, resistance metal part, DCIDC conversion components, high-energy storage equipment.

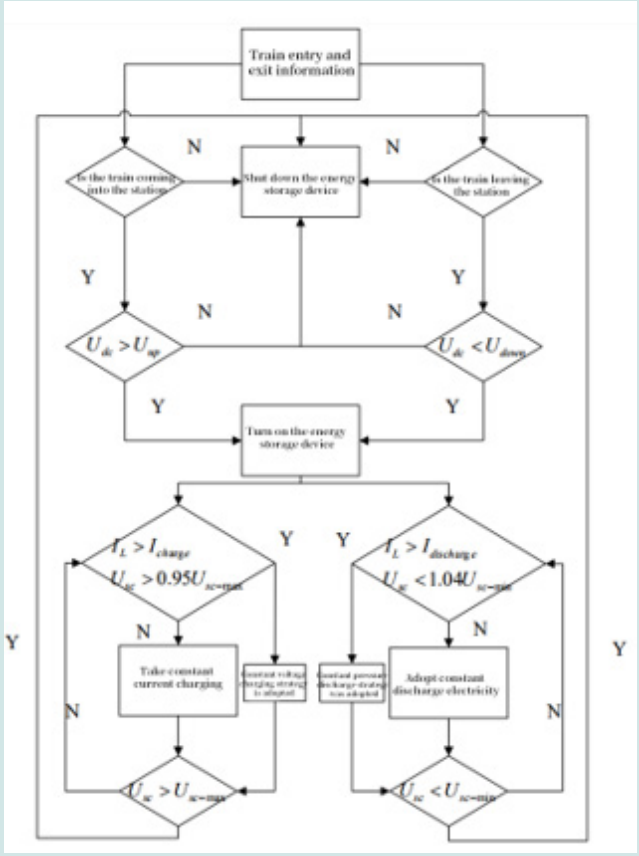

Figure 3: Control strategy of super capacitor energy storage system.

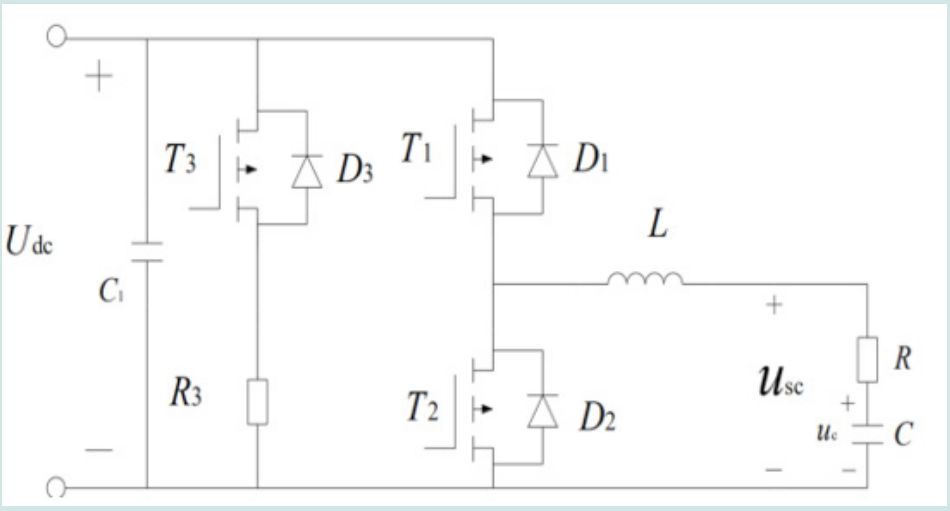

Figure 4: Main circuit diagram of energy storage feedback converter.

Calculation of the Capacity of Supercapacitor Energy Storage System

When calculating the capacity of the super energy storage system, the main basis is the energy released by the city trains during the driving of the bridge. The power of the super capacitor C should ensure that if the power of the main capacitor changes to the maximum, the power of the super capacitor C will change. The energy released is not just the energy stored on the grid when

city trains stop. The city train stopped due to rapid interruption and natural resistance during braking. Natural resistance is divided into normal resistance and resistance to urban orbital movement. The basic resistance is the collision force between the resistance of the train and the air in the moving area. Conflict resistance combines the collision force between the train and the wheels and the resistance between them. The usual resistance formula during operation is:

(6)

In the formula: a, b, c are the resistance coefficients; v is the running speed of the train; g is the acceleration due to gravity; F. is the basic resistance of the train; m is the weight of the train in kg;

The excessive resistance is due to the excessive attraction between the train and the air during operation. There are two types: increased bending resistance and side resistance.

(1) Excessive compression pressure: The extra fraction F is the gravity exerted by the load when the vehicle rises parallel to the bottom of the slope. Its size is equal to one thousandth of the unit weight of the train

(7)

Among them: i is the ramp condition of the line;

m is the weight of the train in kg;

g is the acceleration of gravity;

(2) Excessive bending pressure: Excessive bending resistance F is the shearing force generated when the wheel of the foot contacts the road when the vehicle is driving on a curved road. Calculated as follows:

(8)

Where: D is the diameter of the curve;

m is the weight of the train in kg;

g is the acceleration of gravity;

Therefore, the natural resistance experienced by the train is F = Fw + F1 + F2, and due to the combination of the displacement of the train and the resistance F encountered by the train, the energy W1 of the natural resistance imposed on the train is:

(9)

The weight of the urban train is m and the traveling speed is v. The energy released by the city train from the initial station to the terminal station is:

(10)

Because the size of the super capacitor C must ensure that when the city voltage changes to the minimum and maximum values, the stored energy is much greater than the energy C that can be restored to the city voltage when the city train is stopped. Therefore, the following requirements must be met:

(11)

(12)

Take the DW6L tram as an example. Its average weight is 52t and the maximum speed is 41Km/h. It can be found from the literature that the energy used for the natural resistance of urban trains is about 200 kJ, the conversion efficiency of the energy storage response device is $\alpha = 0.85$, and the low voltage part determines the operation of the super train. Capacitors, up to 400-500V, according to formulas (10) and (12):

(13)

C is 75F; for example, the working value of each supercapacitor is C, and the opposite value of the voltage is U. If the maximum heat capacity of the energy storage system is U and the power is C, the number of m units in series and the parallel groups are:

(14)

(15)

Where: B1 is the ripple coefficient of the inductor current;

IL, is the average value of the inductor current;

Ton is the on-time of the switch tube;

The high voltage value of a single super electric super capacitor is rated as 500F, the voltage protection is 2.5V, and the calculation needs to be connected to 200

After that, 30 groups can be connected in the same way to meet the power requirements of the energy-saving system.

Calculation of Freewheeling Inductance L

In the "buck" state, current flows from the Udc end to the U end of the power supply network. Super capacitor is a kind of energy storage device. The voltage is:

(17)

(18)

In the "boost" mode, it now runs from the Usc terminal in the supercapacitor power supply to the Udc voltage terminal. The voltage and current are:

(19)

(20)

(21)

Where: B1 is the ripple coefficient of the inductor current;

IL is the average value of the inductor current;

Ton is the on-time of the switch tube;

From the above analysis, it can be seen that the free response is related to the Usc voltage through the super capacitor energy storage device, the Udc voltage in the grid, the time flux of the switch tube, the current generation factor and the power factor.

BUCK and BOOST states, calculate the required input values L1 and L2 for each state, and find the maximum value between the two:

(22)

The power supply voltage is 1500V, the frequency of the power supply voltage is 2KHz, D = 0.4, and the current flow rate is less than 0.88. The maximum working voltage is 400V-500V, and the free output is now 100A, then

(23)

(24)

According to formula (19), the required freewheeling inductance can be calculated to be 2.5mH.

Calculation of Stabilized Capacitor C1

The working state of the backup DC/DC converter can be divided into two types: one is the working state of BUCK, and the other is the working state of BOOST. Due to the presence of super capacitors, the step-down region has a special filtering function, so there is no need to add additional power. In the BOOST area, the voltage fluctuation in the filter device is the voltage value in the generator, which is recorded as AU. Meet the requirements of the following formula:

(25)

In the formula, fc is the cut-off frequency of the filter circuit, and there are:

(26)

After the "BOOST" mode, the device size filter capacitance value is:

(27)

In the BOOST mode calculated in the upper half, f = 2KHz, usc = 500 V, AU, = 15V and L = 2.5mH, the BOOST port can be used to lock the card:

(28)

Selection of Switch Tube

The main problems that need to be solved when choosing a power supply are the switching frequency, the excess power that is ultimately turned off, and the voltage that is allowed to pass when it is turned on. Nowadays, the equipment widely used to replace electrical and electronic equipment includes turn-off thyristors, power transistors, electric effect transistors, and transistor radian insulated bipolar transistors.

a) Shut-off Thyristor:

Shut-off thyristor is an advanced self-extinguishing device with three ports: gate, cathode, and anode. The gate controls the opening and closing of the cathode and anode. It has the characteristics of large wind tunnel, low pipeline voltage and high-pressure resistance, but the signal trigger door must have sufficient driving power, long turning time and frequent movement time.

b) Power Transistor:

Power transistors, also known as giant transistors, have a base, emitter and collector. It has a high flow rate and high-pressure resistance. Now it is a controlled tool like GTO. The driver needs a lot of things to drive and shut down, but the transmission frequency is much higher than GTO. Usually used in small and medium-sized conversion equipment, it has been gradually replaced by IGBT and POWERMOSFET.

c) Electric Effect Transistor:

An electric effect transistor has a gate, a source, and a drain. There is a network that can turn off the transistor effect in the control point and power zone. It is an electrical control device. Compared with the previous two models, its driving ability is small, can reach a very high frequency, and the power is strong. Transistor radian insulated bipolar tube: Transistor radian insulated bipolar tube has gate, emitter, and collector. Dual-core transistors are part of a fully controlled electrical device composed of two-dimensional transmitters and effective gate transistors. If both DC/DC switch sides are running on BUCK and BOOST, the maximum voltage on both sides of the T1 and T2 pipelines is a net power supply of 1500V. If 50%-60% of the rated voltage is used, the output power is 3000V for the IGBT. If the T1 and T2 tubes are used as transmission tubes, the current flow rate is the charge and current release of the supercapacitor. If possible, set t to 20s according to the power balance relationship.

(29)

According to formula (29), the average current flowing through the T1 tube and the T2 tube can be obtained:

(30)

If used as half of the current rating, the rated current is 400A. If you choose IGBT, you can choose Infineon IGW60T120FKSA1 model (rated voltage is 1200V, alternating current is 2-20KHz, now rated as 100A), the group size is 2.

Construction of the Simulation Platform

Model of Traction Substation

In the urban railway operation system, the power station is responsible for reducing and adjusting the three-phase switch to the direct voltage of 1500V or 750V DC, and is responsible for the operation of the train through the power supply and the power grid. It can be adjusted using a three-phase power system and 24 pulses. As shown in Figure 5: a three-phase electrical system, the system is adjusted to release DC power to supply power to the load after a 24-stroke center adjustment.

Train Model

In urban traffic, traction motors provide power for trains. In my country's urban railways, motors usually use three-phase

asynchronous AC motors and a set of reciprocating devices to restore DC power. This is a three-phase continuous circuit designed for current conversion engines. In simulation, the train model can be compared with the combination of switchgear and AC three-phase motor, and the start and stop of the three-phase motor can be controlled to match the working conditions of city trains. This example is shown in Figure 6 below.

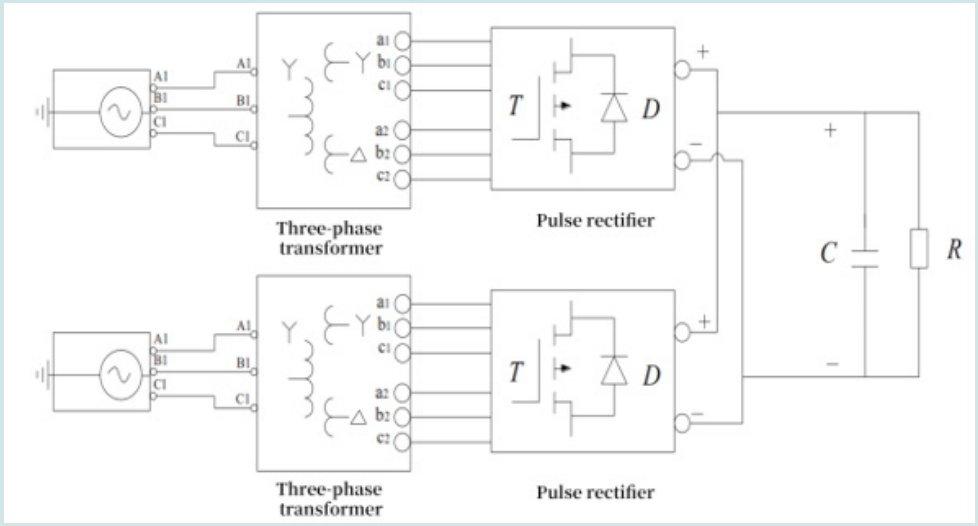

Figure 5: Traction substation module.

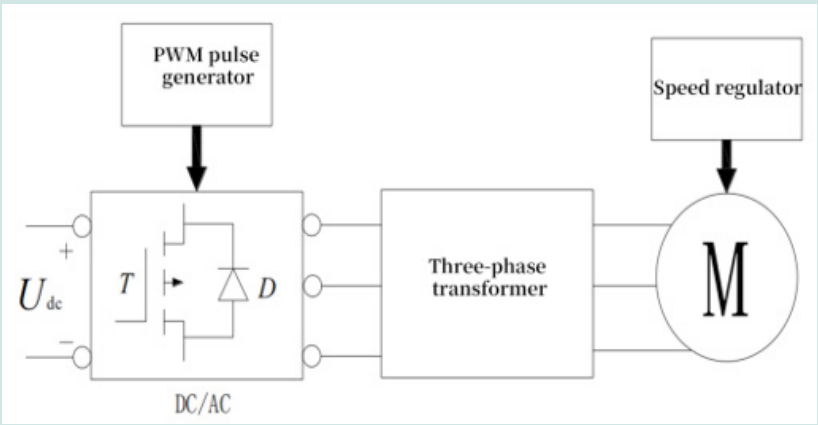

Figure 6: Train model.

Supercapacitor Energy Storage System Model

The power storage system is usually composed of a series of mxn supercapacitors in parallel, and some circuits for controlling the same voltage are added externally. Under the simulation conditions, the voltage control of the same power can be ignored, and the corresponding sum can be obtained, and then the appropriate capacitor plus the same series resistance can be applied to the same model of the supercapacitor energy storage system. The specific structure of the storage capacity storage system is shown in Figure 7. From the calculation results in the previous section, it can be seen that by connecting 200 series units with 500F, and then connecting 30 identical groups, an energy storage system can be obtained. Therefore, the energy storage system can be equivalent to a period of C=75F and R=3mΩ.

Overall Model of Supercapacitor Energy Storage System

Combine the two sides of the DC/DC switch in the first part to obtain the general structure of the energy storage system, as shown in Figure 8. In this circuit, the PWM control signal part detects the power grid and the train data. If a city train enters a station and the brake or city train starts to leave the station, and the line network voltage meets the electric storage device, the electric storage device is activated to charge the energy captured by the outgoing train. And the energy released by the brake on the grid will be absorbed and stored. The control unit in the first part manages the energy storage and release of the supercapacitor energy storage device by controlling the charge and current release of the freewheeling inductor and the voltage on the entire energy storage device.

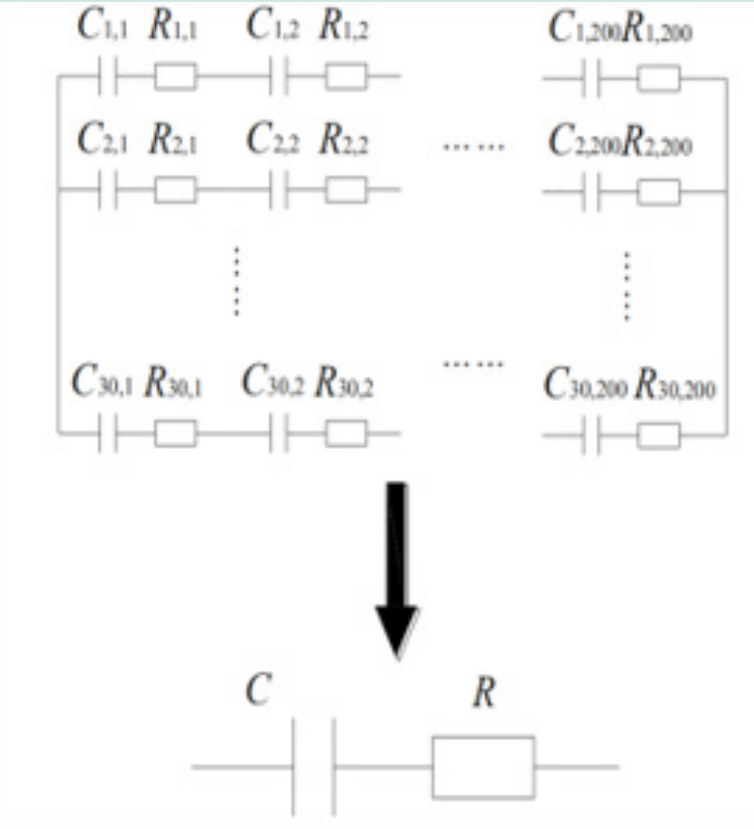

Figure 7: Supercapacitor energy storage system model.

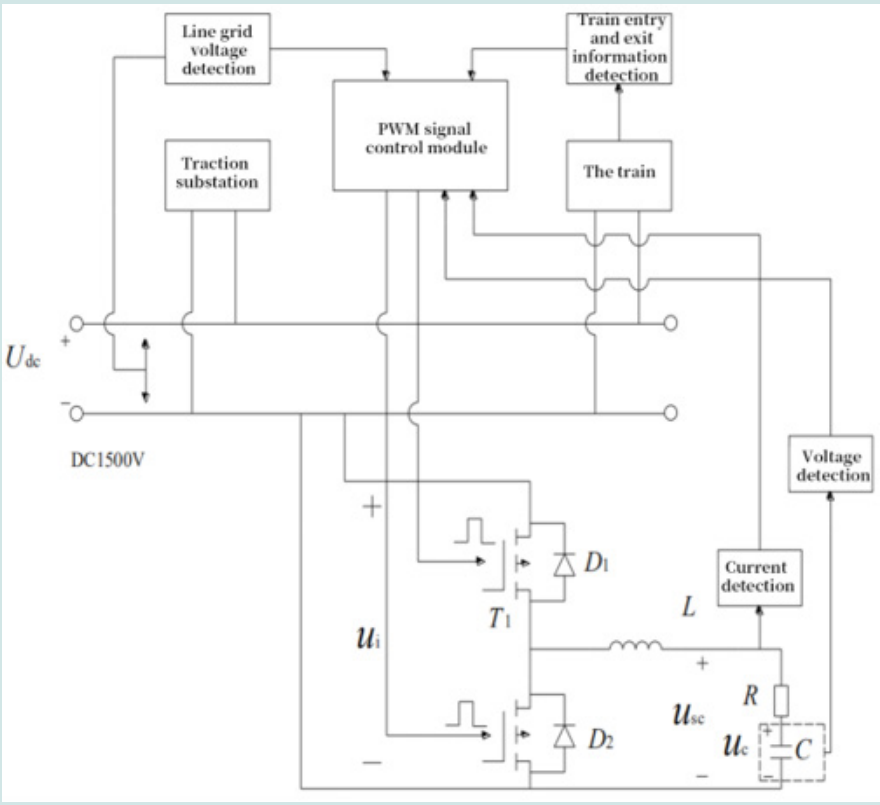

Figure 8: The overall model of the super capacitor energy storage system.

Analysis of Simulation Results

In the simulation part of the previous part, the system was modeled as MATLAB/SIMULINK. The simulation diagram is shown in Figure 9. On the right side of the hypothetical diagram is the main circuit of the supercapacitor energy storage system, which is mainly connected to the speed base. The design and structure of the track, the structure of the power storage system, the storage system of the connecting rod and the control system to achieve this function; the measurement results have two simulation experiment components: one is the change of the power grid before and after the high-energy storage system starts when the train leaves the station , And the experimental energy storage of the two ends of the energy storage system and the current; the second is the electrical simulation test of the super capacitor energy storage system through the station to transport the power grid before and after the train is activated, the power grid on both sides of the system to save energy, and to continue Flow current generator simulation test. According to the results of the comparative simulation, the working conditions of the energy storage system were checked, and the influence of the energy storage system on the increase and decrease of power in the power supply network was studied. Since the traction of the city train runs inside the motor, the urban rail transit system can be controlled by controlling the speed of the motor. The vehicle speed is increased from 0r/min to 1400r/min and from 10s to 30s. The system is used to simulate the initial mode of urban railways. From 30s to 50s, the speed is maintained at 1400r/min, which is a uniform motion. Reduced from 50 seconds to 70 seconds, reduced to or/ min, used for the same as the city train stopping system; Figure 10 below shows the change of city train speed. Includes supercapacitors that store energy in the device. The device contains a feedback super capacitor, releases energy, and releases network power to provide part of the power required to start the train. The energy carried by the grid is reduced in the same way. Currently, the electric field voltage reaches 1400V Figure 11. When the train stops, the superpower steering device used for braking absorbs the energy released when the train stops in a city train. When the train is braking, the energy released by the power supply network will be reduced accordingly. At this time, the voltage increased to 1620V.The transmission and release current of the supercapacitor storage capacitor during operation is shown in Figure 12. It can be seen from the curved curve that the Uac network gateway drops to the set value within 20 seconds, and Udown = 1450V after storing the high power. If the power supply is changed, the super capacitor system can save the cost of the power supply network. The DC/DC binary switch will operate in the BOOST area. The positive direction of the current is determined by the flow from the grid to the supercapacitor. Therefore, the maximum current used by the energy storage device is -180A. Now it supplies power to the power network. After 60 seconds, UDC's charging cost is set to Uup = 1550V, high-turning electric energy storage, and the two stages of the DC/DC Buck area are working hard to make urban railway trains more stable. In terms of energy generated, the power supply network provides a maximum current of 100A for energy-saving equipment. The command and output voltage of the super capacitor voltage generator during operation are shown in Figure 13. It can be seen from the current-voltage curve that within 20s, when the two bidirectional converters DC/DC are operating in the output state. At -180A, the voltage through the supercapacitor began to drop to 480V, until the voltage in the power network returned to normal after 37s, the energy storage equipment of the supercapacitor gradually stopped distributing power to the power supply network. The power and voltage of all energy storage devices are reduced to 425V; 60s if the DC/DC dual switch is working in the charging state, if the current voltage changes from 0 to 100A, the voltage to the mains voltage will start to rise from 425V until the voltage normal. The power network will stop generating super capacitor energy, and the voltage of all energy storage devices will rise to 462V.

Empirical Analysis of Train Operation

Under speed conditions, the initial acceleration is 0.905m/s2. The constant acceleration area under braking is 0.79 m/s2, and at the same time, it gradually changes to air brake at a speed of 3km/h. Table 2 shows the parameters of the test train on a certain line.

Table 2: SD card SPI mode pin definition.

Parameter	Numerical value	parameter	Numerical value
Train formation	3M3T	Motor rated power	180 kW
Traction network (third rail) rated voltage	750 V	Auxiliary power supply capacity and number	160 kVAx2
Load power factor	0.85	Inverter efficiency	0.93
Maximum train acceleration	1 m/s2	Motor efficiency	0.915
Maximum train deceleration	1 m/s2	Gear efficiency	0.975
Maximum speed limit	80 km/h	Electric brake adhesion coefficient	≤0.16
Braking resistor resistance	1.23 Q	Braking resistor start threshold	920 V
Average acceleration	N0.84	Brake deceleration	0.83
0~40km/h average acceleration	N0.83	0~80km/h average acceleration	≥0.5

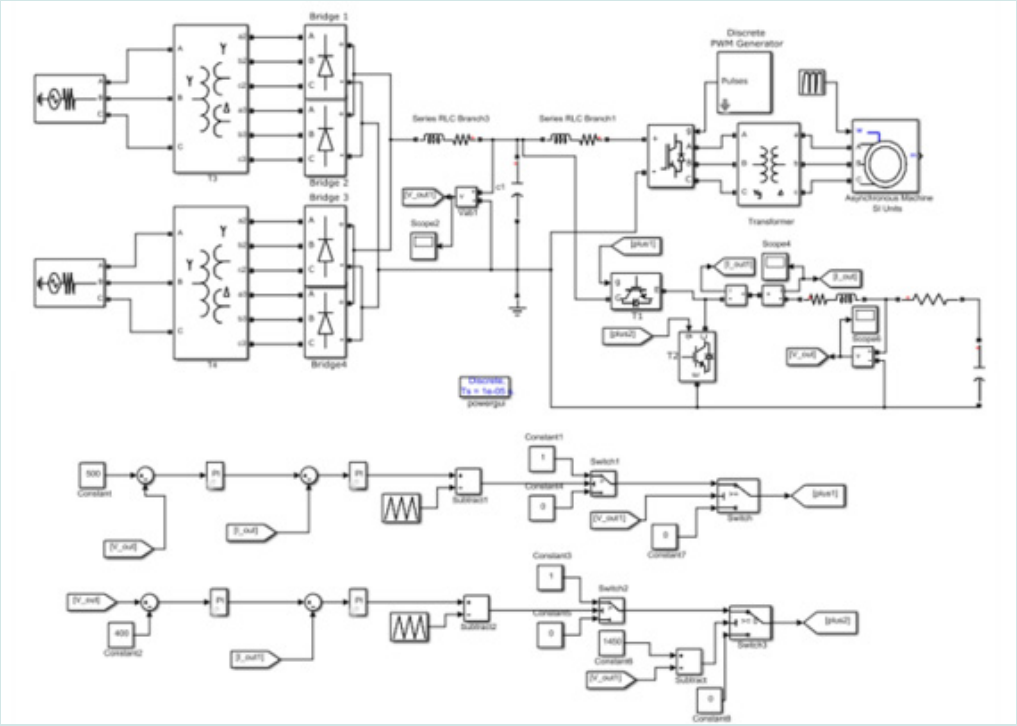

Figure 9: Schematic diagram of the overall simulation of the super capacitor energy storage system.

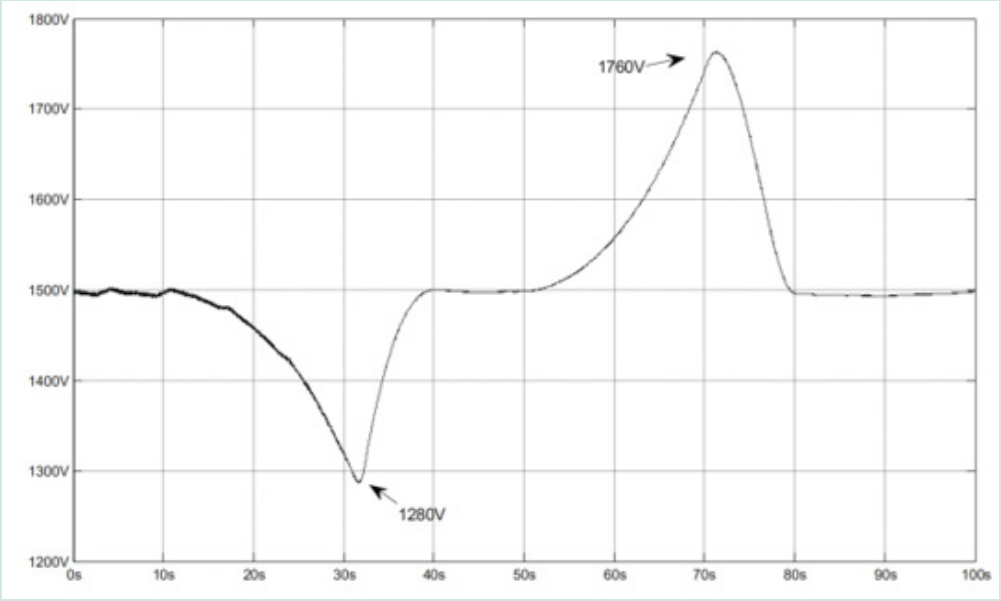

Figure 10: The impact on the voltage of the power supply network when the train starts and brakes without the energy storage device.

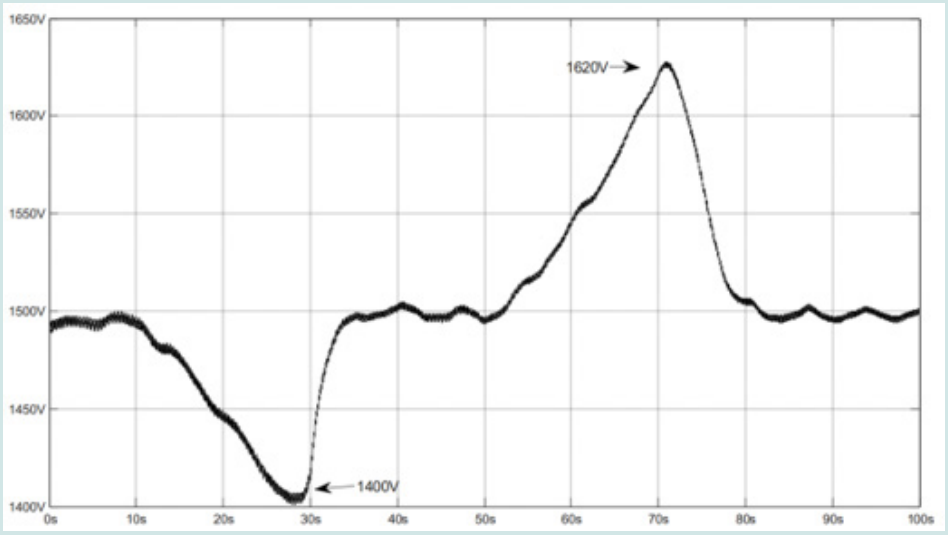

Figure 11: The impact on the voltage of the power supply network when the energy storage device is added to the starting and braking of the train.

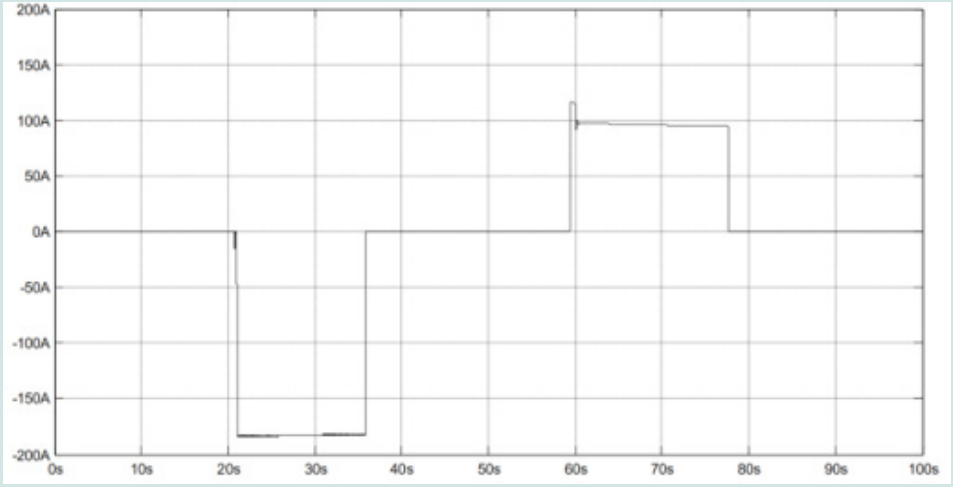

Figure 12: The charging and discharging current curve when the train is braking and starting.

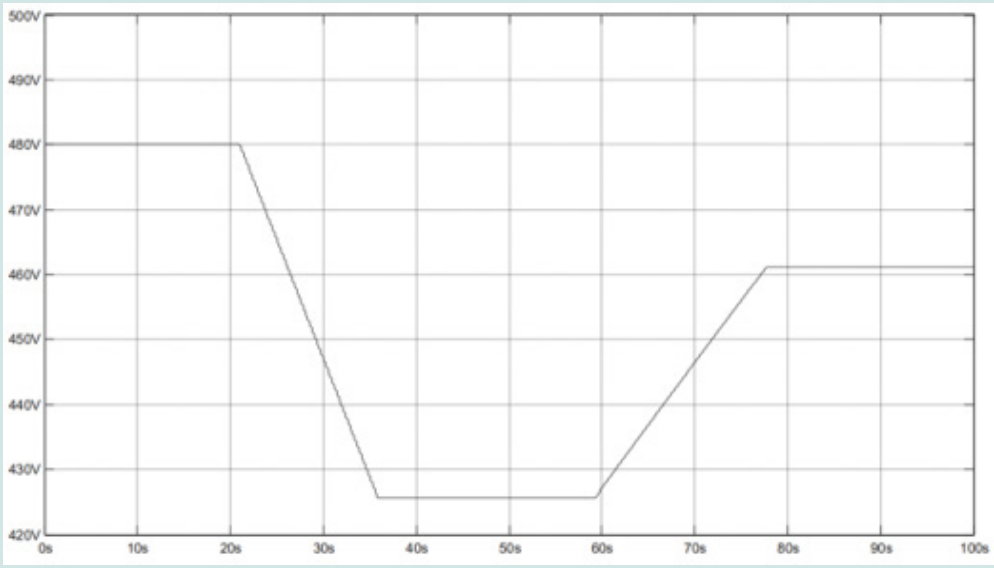

Figure 13: The change curve of charging and discharging voltage when the train is braking and starting.

Parameters of 1Mw Super Capacitor Energy Storage System

The super capacitor high energy storage system is composed of 48 V / 165 F super MAXWELL modules. The module is composed of 2.7 V / 3000 F monomer. The module receives a 1Mw super capacitor power storage system through 14 series and 10 parallel, and the internal resistance of each component is 6.3 mQ. The specific limits of energy storage equipment are shown in Table 3.

Table 3: Energy storage system parameters.

Parameter	Numerical value	Parameter	Numerical value
Input voltage	500-1000 V	Total capacitance forging	117.9 V
Input filter capacitor	15 ml	Maximum operating voltage of capacitor	672 V
The output voltage	0-600 V	Internal resistance	8.82 mQ
Rated output current	2000 A	Energy storage	7.4 kWh
Number of modules connected in series	14	Number of modules in parallel	10

A Certain Line Test Verification of Train Operation Adjustment Strategy

It can be seen from the above that, no matter it is current or voltage, compared with the curve before adjustment, the change of the curve after correction is reduced. Before adjustment, the voltage between charging and discharging the supercapacitor 260 is 580 V, and the current voltage is -310~330 A; after adjusting the curve, the voltage of the high voltage transformer is 290~570 V, and the current rating is -310~300A. Since the adjusted train control energy will not be absorbed from nearby trains, in addition to losing the self-service of trains and lines, it will also return to the energy storage device for charging. The statistics before and after the adjustment are shown in Table 4. Accordingly, the energy release of the supercapacitor before and after maintenance is reduced. By comparing the charged power, it can be found that after the train operation and maintenance, the thermal power of the supercapacitor is reduced by 9.17% compared with the previous maintenance, that is, improving the operating conditions of the train can increase the speed between the connected trains by 9.17%. The statistical data before and after the adjustment is shown in Table 5.

Table 4: Supercapacitor charge and discharge energy statistics before and after the first set of adjustments in the train operation adjustment test.

Super capacitor energy	Charging energy (kWh)	Discharge energy (kWh)
before fixing	2.6458	2.274
adjusted	2.334	1.813

Table 5: Supercapacitor charge and discharge energy statistics before and after the second set of adjustments in the train operation adjustment test.

Super capacitor energy	Charging energy (kWh)	Discharge energy (kWh)
Before fixing	1.7	2.063
adjusted	1.544	2.0447

Octopus Line Test Verification of Charging Control Strategy for Supercapacitor Energy Storage Device

Count the energy of the six sets of test substations, trains and energy storage systems, as shown. At the same time, it is defined that the energy saving n is the ratio of the discharge energy of the energy storage device to the output energy of the substation. The experimental data is shown in Table 6:

Table 6: Energy statistics table in the dual train operation test.

Test grouping	SC discharge energy (kWh)	SC discharge energy (kWh)	Substation energy (kWh)	Train energy (kWh)	Energy saving rate n
1	1.73	4.5	22.1	23.83	7.30
2	3.98	4.44	29.31	33.29	12
3	4	3.45	12.67	16.67	24
4	4.32	3.89	16.67	20.99	21
5	3.6	4.55	13.85	17.45	20.6
6	4.14	3.88	15.07	19.21	21.6

It can be seen from the following four sets of experiments that using the proposed control strategy, the average energy storage rate of the energy storage device can reach 21.7%. Compared with the average energy saving of 9.65% of the first two groups of fixed flow control strategies, the energy storage rate has increased by 12%, that is, the energy consumption rate of the regenerative energy stored in the energy storage system has increased by 12%, and the power of the super capacitor.

Conclusion

This article takes the error analysis of the railway transmission system as an application program, which often drives the design of equipment and software development. This is the most important part of accessing Web monitoring tools and performance, that is, the work of the software and the device driver, which are compatible with DSP and FPGA. See train entry and exit information. When the power supply rises and drops to the set value, the super capacitor energy storage device starts to work, and a simulation platform that meets the super energy demand of the energy storage system is established. It also provides a simulation platform for super energy storage and an energy storage response control system. When trying to change the operation of the train, you need to consider the upper and lower trains at the same time and use the ground energy storage system to perform energy statistics before and after the train. The results of the comparison of the two types of experiments were statistically improved, and the energy storage rates of the front and rear wheels were increased by 11.7% and 9.17%, respectively. Experiments have shown that the increase in the power of the adjusted train is due to the decrease in train operation changes and the decrease in voltage changes, which confirms the purpose of improving train performance.

References

1. Messing R, Pal C, Kautz H (2009) Activity recognition using the velocity histories of tracked keypoints. In: Proceedings of the IEEE International Conference on Computer Vision pp. 104-111.
2. Messing R, Pal C, Kautz H (2019) University of Rochester activities of daily living dataset.
3. Choi W, Shahid K, Savarese S (2009) What are they doing? Collective activity classification using spatio-temporal relationship among people. In 2009 IEEE 12th International Conference on Computer Vision Work ICCV Work 24(1): 1282-1289.
4. Choi W, Shahid K, Savarese S (2019) Collective activity dataset.
5. Project B (2019) Computer-assisted prescreening of video streams for unusual activities.
6. Singh S, Velastin S A, Ragheb H (2010) MuHAVi: A multicamera human action video dataset for the evaluation of action recognition methods. In: Proceedings-IEEE International Conference on Advanced Video and Signal Based Surveillance pp. 48-55.
7. Murtaza F, Yousaf MH, Velastin SA (2016) Multi-view human action recognition using 2D motion templates based on MHIs and their HOG description. IET Comput 10(7): 758-767.
8. Singh S, Velastin S A, Ragheb H (2019) MuHAVi: multicamera human action video data.
9. Ryoo MS, Aggarwal JK, Chen C, Roy Chowdhury A (2010) An overview of contest on semantic description of human activities (SDHA). In ICPR contests pp. 270-285.
10. Ryoo MS, Aggarwal JK (2009) Spatio-temporal relationship match: video structure comparison for recognition of complex human activities. In: Proceedings of the IEEE International Conference on Computer Vision pp. 1593-1600.
11. Ryoo MS, Aggarwal JK, Chen C, Roy chowdhury A (2019) ICPR 2010 contest on semantic description of human activities (SDHA 2010).
12. Chen C, Aggarwal JK (2009) Recognizing human action from a far field of view the University of Texas at Austin. In Analysis pp. 1-7.
13. Chen CC, Ryoo MS, Aggarwal JK (2010) UT-tower dataset: aerial view activity classification challenge.
14. Sangmin Oh, Anthony Hoogs, Amitha Perera, Naresh Cuntoor, Chia Chih Chen, et al. (2011) AVSS 2011 demo session: a large-scale benchmark dataset for event recognition in surveillance video. Video Signal Based Surveillance 2(1): 527-528.
15. Oh S (2019) VIRAT video dataset.
16. Gehrig D, Peter Krauthausen, Lukas Rybok, Hildegard Kuehne, Uwe D Hanebeck et al. (2011) Combined intention, activity, and motion recognition for a humanoid household robot. In IEEE International Conference on Intelligent Robots and Systems pp. 4819-4825.
17. Gehrig D (2019) The Karlsruhe Motion, Intention, and Activity Data set (MINTA).
18. Rybok L, Friedberger S, Hanebeck U D, Stiefelhagen R (2011) The KIT Robo-Kitchen Activity Data Set.
19. Ivan L, Marszałek M, Schmid C, Rozenfeld B (2008) IRISA/INRIA Rennes France: learning human actions from movies p. 1-8.
20. Marszałek M, Laptev I, Schmid C (2009) Actions in context. In 2009 IEEE Computer Society Conference on Computer Vision and Pattern Recognition Work CVPR Work pp. 2929-2936.

DOI: 10.32474/CTCSA.2023.03.000151